ADVANCED RESEARCH PROGRAMS IN TURBOMACHINERY

by

Dr. Meherwan P. Boyce

Director, Gas Turbine Laboratories

Texas A&M University

College Station, Texas

William L. Trevillion

and

Michael L. Brown

Graduate Research Assistants

Gas Turbine Laboratories

Texas A&M University

College Station, Texas

Dr. Meherwan P. Boyce, director of the Gas Turbine Laboratories, is an associate professor of mechanical engineering at Texas A&M University. He is a consultant for a number of major manufacturers and users of turbomachines. He was the only U.S. delegate invited to the IV USSR Compressor Conference. He is chairman of the Technical Resources Committee of the Gas Turbine Division of ASME and the 1975 program chairman for the 20th Annual International Gas Turbine Conference. He is also chairman and founder of the Turbomachinery Symposium held annually at Texas A&M University. Dr. Boyce received a Bachelor's degree from South Dakota School of Mines and Technology; a Master's degree from the State University of New York; and a Ph.D. from the University of Oklahoma. Before joining the academic community, he was in charge of the compressor development group at Curtiss-Wright Corporation, and was group leader of the aerodynamic groups at Fairchild Hiller Corporation-Stratos Division. His numerous writings on turbomachinery and fluid mechanics have set some basic design parameters.

Dr. Boyce was the recipient of the 1973 Ralph Teetor Award from the Society of Automotive Engineers and also holds the 1974 Herbert Allen Award from The American Society of Mechanical Engineers. He is a member of several scientific and engineering honor societies. He is a registered professional engineer (Texas).

William L. Trevillion is a senior research assistant with the Laboratories, and is an instructor in the Mechanical Engineering Department. He received his Bachelor of Science degree and his Master of Science degree in Mechanical Engineering from Texas A&M University. He is presently working on his doctorate. He served in the Marine Corps for seven years and held the position of captain at the time of his discharge. He has extensive practical experience in the area of jet engines, and he has worked in the area of axial flow compressors. He is a member of ASME and SAE.

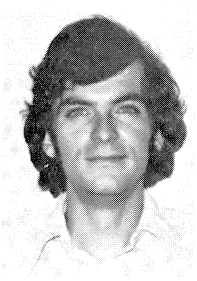

Michael L. Brown is a research assistant with the Laboratories. He graduated from the Georgia Institute of Technology in 1973 with a BSME degree. He worked in the Gas Turbine Division of Caterpillar Tractor Company as research engineer until coming to Texas A&M University, where he is presently working on his Master of Science degree in Mechanical Engineering. His work involves combustion and fuels. He is a member of ASME, SAE, and Pi Tau Sigma.

ABSTRACT

The objective of this paper is to acquaint the reader with the developments in the field of turbomachinery. The research conducted at the Gas Turbine Laboratories has two primary goals. First, to improve the efficiency of high speed rotating machinery, and secondly, to increase the reliability of the system. This paper covers both areas by looking into the improvement in characteristics of centrifugal compressors and combustors; and by dealing with the maintainability and reliability of high speed turbomachinery.

The paper deals with various techniques developed at the Laboratories to describe the flow in centrifugal impellers. Once the flow patterns in a compressor are known, various concepts can be utilized to improve the efficiency. One such concept is the tandem inducer described here. This concept shows an increase in the efficiency and surge-to-stall margin. This concept also indicates that the traditional positioning of the splitter blades is not optimum. Combustors designed with high efficiency and low emission characteristics are also described here. Multiple fuel characteristics and their effect on turbine life, and other maintenance characteristics are further described here in detail.

INTRODUCTION

Turbomachinery research and development programs span across a large specturm of concepts from bearings and seals to compressor and turbine programs. The major research and development programs undertaken deal with component improvement. In this paper we will examine techniques which can be used to improve the efficiency of centrifugal compressors and surge-to-stall margin.

Combustor design to improve efficiency and reduce NO_x output is an area which is getting a lot of attention. The research conducted in this area deals not only with gaseous fuel but with distillate fuels as well.

Maintenance and reliability techniques have been developed over the years, which can be used to plan and schedule major and minor overhauls. The programs described here are conducted at the Gas Turbine Laboratories as a continuing service to the turbomachinery community.

COMPRESSORS

The flow in a centrifugal compressor is an extremely complex phenomenon, affected by the geometry of the compressor, the viscosity and density of the fluid passing through the compressor, and the energy gradients produced in the fluid by the compressor. The change of the direction of flow from an axial entry to a radial exit makes the flow more complex. This highly complicated flow is strongly affected by three-dimensional boundary layers on blade surfaces, secondary flows in blade passages, and flow separation from solid boundaries.

The flow in centrifugal impellers has been described analytically by various investigators such as Katsanis (1), Boyce and Bale (2), and Senoo and Nakase (3,4). The three-dimensional solutions assume, in general, the flow to be inviscid and that it follows the blade surface. These are the quasi-three-dimensional flow solutions, and are obtained by superimposing the two-dimensional solution of the hub-to-shroud plane upon the blade-to-blade plane solution for the radial bladed impellers. These solutions do not describe the flow very accurately, especially at the blade tip. However, they do indicate flow tendencies, and thus are helpful to the designer. Viscous solutions have been considered by Bale (5), however, these solutions need further refinement.

Flow Visualization

Experimental investigations have been conducted by Boyce (6), and Fowler (7,8) in which the flow through model impellers was visualized. Boyce employed a small impeller in which water was the working fluid; and Fowler used an extremely large impeller which rotated at a slow velocity. Bammert and Rautenberg (9), Gorton and Lakshminarayana (10), Mizuki, Ariga, and Watanabe (11), and Eckardt (12) measured the real flow phenomenon with instantaneous measurement techniques.

While extremely hard to understand, the flow in centrifugal impellers is a very important area of research in the area of improving compressor and gas turbine performance. The compressor efficiency has the strongest influence on fuel consumption of the gas turbine among its components. A three percent gain in compressor efficiency leads to approximately a three percent reduction in fuel consumption. Because of the importance of centrifugal compressors, the majority of the research conducted by the Gas Turbine Laboratories in the previous year, has been directed toward finding methods for improving the performance of centrifugal impellers.

This lack of understanding of flow is a severe handicap in the design of centrifugal impellers. More must be understood about this flow if the aims of high pressure ratios per stage, high efficiency, and large surge-to-stall margins are to be obtained. The current theoretical methods fail in analyzing the flow near critical flow areas, such as blade tips, blade edges, and at points of flow reversals. It is these locations where the greatest losses occur and stall is initiated. Flow reversals cause separation in impeller passages with resulting eddy losses, mixing losses, and changed flow angles. This separation should be avoided or at least delayed to improve compressor performance. More must be learned about the flow in impellers if this reversal and separation is to be prevented, or its effects lessened.

In order to obtain a better understanding of flow in impeller passages, flow visualization has been a major project of the Gas Turbine Laboratories. A model centrifugal impeller was designed and constructed for hydraulic analogy studies. The impeller hub and blades were made of aluminum and constructed separately, as shown in Figure 1. The hub was machined to provide the proper profile, and then the interior machined to form a hollow-shell. The blades were drilled and tapped, then attached to the hub by bolts extending through holes in the hub. This method of attaching the blades permits experiments with different blade designs. The number or shape of blades can be easily and quickly changed. The impeller design selected for the initial experiments is shown in Figure 2. The blade shape provides a flow which slightly decreases toward the exit to provide the proper pressure gradient. An inlet blade angle of 20° was chosen for the inducer to match the velocity triangles at the mid-point of the leading edge of blades. The impeller was mounted inside a plexiglass shroud. The inlet pipe leading to the shroud and diffuser plates were also made of plexiglass to permit observation of the flow throughout its passage in the impeller. The impeller was mounted onto a steel table by two bearings. The table containing the impeller shroud and diffuser was placed in a tank which served as the drain tank for water exiting the diffuser. The impeller was rotated through a pulley system, by a variable

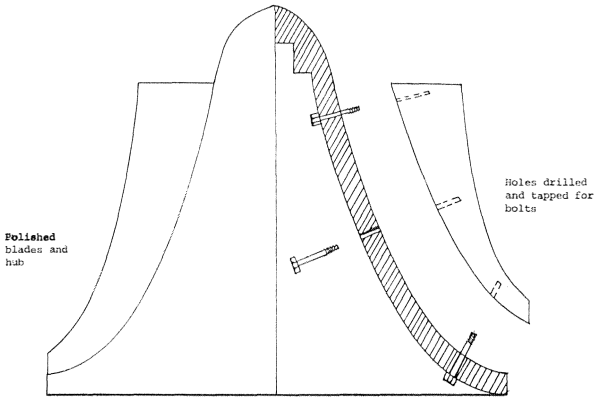

Figure 1. Blade Mounting System.

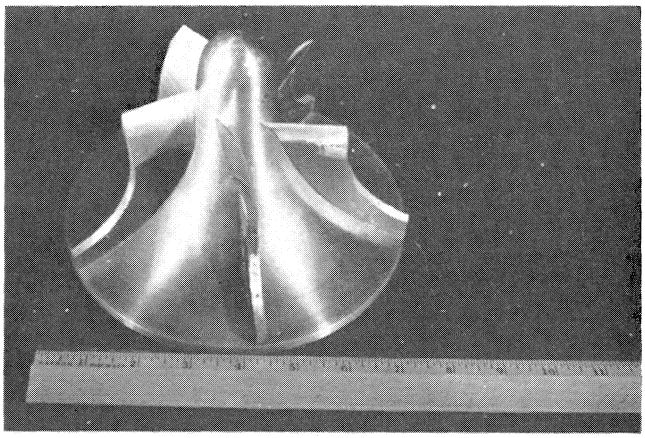

Figure 2. Assembled Impeller.

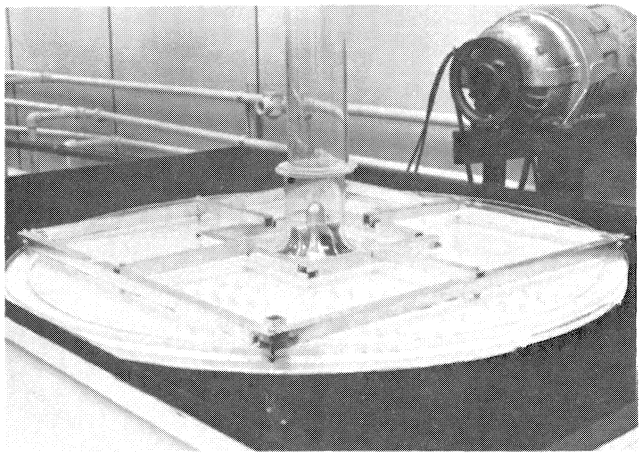

Figure 3. Assembled Flow Model.

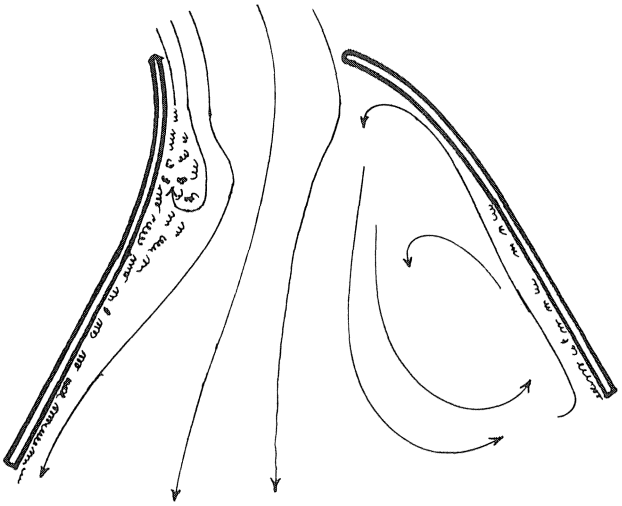

Figure 4. Streamlines Near the Impeller Hub.

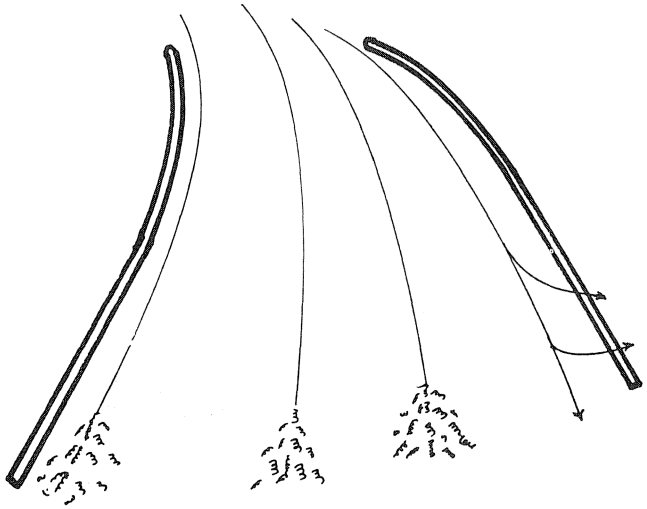

Figure 5. Streamlines Along the Impeller Shroud.

speed motor mounted above the drain tank. The diffuser was held in place by square tubing. Figure 3 is a photograph of the completed assembly.

The impeller was rotated and dye injected into the water at the impeller entrance. The dye which was a neutral density mixture of kerosene, dibutyl phthalate, and black paint,

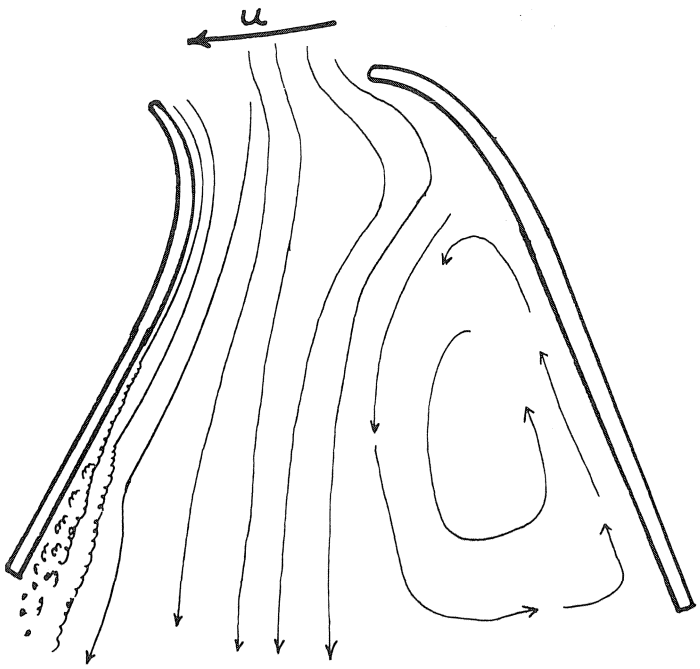

Figure 6. Streamlines in the Central Portion of the Meridional Plane.

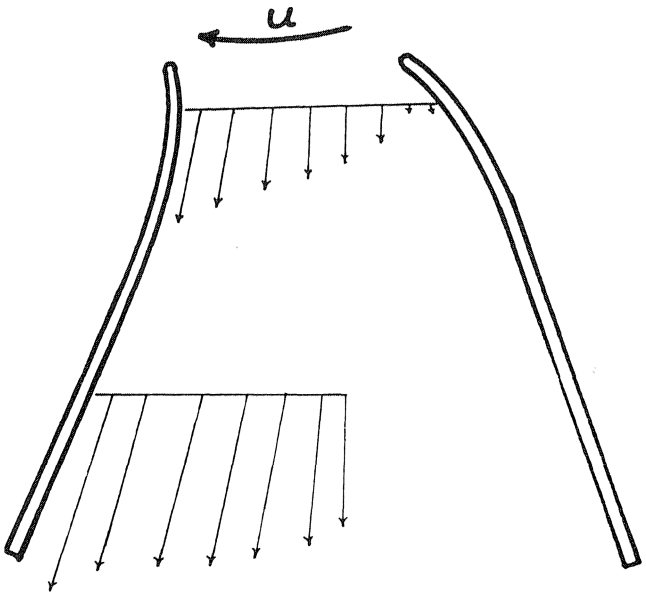

Figure 7. Relative Flow Velocities.

formed globules when injected into the flow stream. High speed motion pictures were taken of the flow and then studied to obtain a map of flow through the impeller. The image of the dye could be used to determine the distance of the dye from the impeller surface and therefore, provide a three-dimensional map of the flow. The streamlines were obtained first, by tracing the flow through the passages, and then the velocities obtained by comparing the distances travelled during a certain number of frames. The streamlines along the hub, shroud, and the central portion of the passage are shown in Figures 4, 5, and 6, respectively. Figure 7 shows the velocities of flow in the central portion of the meridional plane.

The streamlines show a large stagnation area near the pressure surface, just past the inducer section. This stagnation area caused flow entering the impeller passage near the pres-

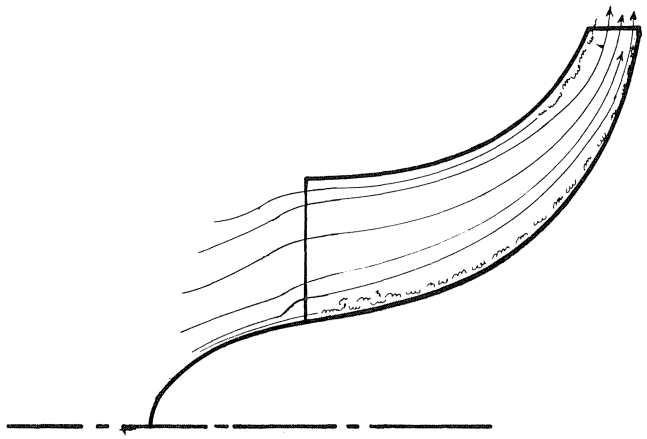

Figure 8. Streamlines on the Meridional Plane Along the Suction Surface.

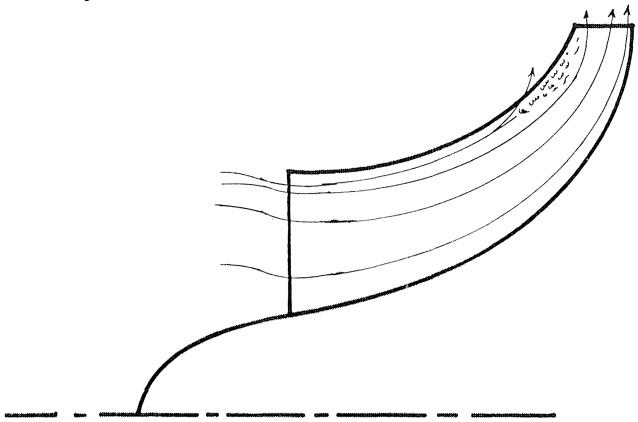

Figure 9. Streamlines on the Meridional Plane Along the Pressure Surface.

sure surface of the blades to slow, then flow toward the suction surface of the blades, and finally, turn again and flow toward the impeller exit. Figures 8 and 9 show the flow in the meridional plane near the suction and pressure surfaces of the blades. It is these results which led us to our program of a tandem inducer. These results agree very closely with results obtained in flow studies with impellers employing air as the working fluid.

More date regarding the effect of splitters, blade tips, suction, etc. will be collected from future experiments with this or similar impellers. In this manner it is our goal to increase the efficiency of the impeller and to increase the surge-to-stall margin.

Tandem Inducers

Results obtained from the flow visualization work, led to a program to improve the performance of centrifugal impellers by modifying the inducer section of an impeller. Experiments conducted by Balje (13), in which a tandem arrangement of cascades was studied, showed less profile losses than with plain cascades.

Prithvi Raj and Narayanan (14) applied this principle to a centrifugal impeller, by splitting the vanes, and obtained efficiency increases in low flow coefficient range. The research undertaken by the Laboratories used theoretical and experimental investigations of flow in a centrifugal impeller with a modified tandem inducer to gain a possible reduction of flow separation. This modification was conceived with the theory that the tandem inducer blades could give additional kinetic energy to the boundary layer and it would be less likely to separate.

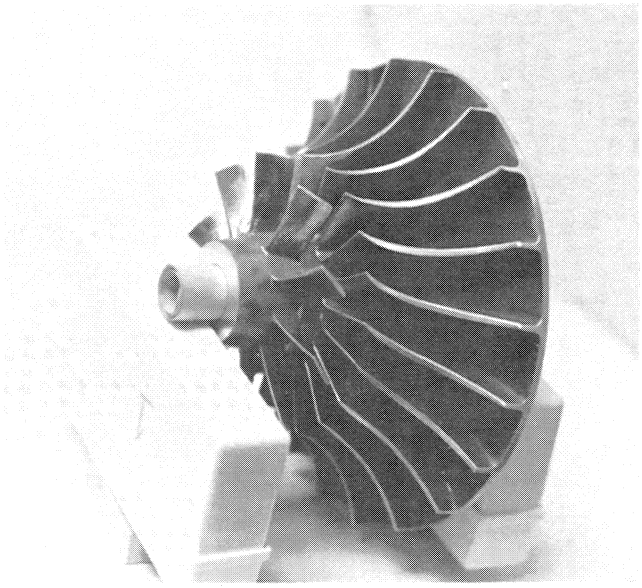

Figure 10. Impeller With Offset Inducer.

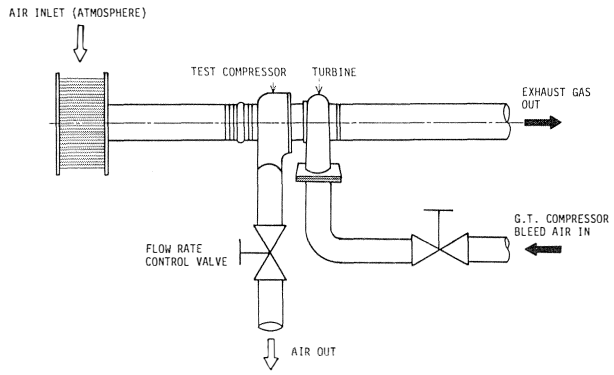

Figure 11. Schematic of Test Facility.

In the theoretical portion of this program, calculations were performed with a quasi-three-dimensional method to obtain a solution of through-flow outside the boundary layers on the surfaces of the blades. The boundary layer solution was then obtained by solving the Navier-Stokes equation along both blade surfaces within the axial inducer. Both solutions were then combined to investigate the entire flow in the tandem inducer.

The experimental portion of the research was conducted by modifying the impeller of a turbocharger. The impeller was cut at the rear of the inducer section, and the inducer rotated relative to the remainder of the impeller. The inducer was locked in this position and tests run with the inducer in this position as shown in Figure 10. The turbocharger was powered by the bleed air from a Garrett gas turbine. The rotational velocity was controlled by a valve, and the flow through the compressor was also controlled by a valve, as shown in Figure 11. Total pressure rake probes were installed at the compressor inlet and the discharge duct. The pressures were indicated on manometers and the temperature, at the compressor inlet and discharge obtained from thermocouples. Figure 12 shows the schematic of the instrumentation arrangement. The impeller speed was obtained by means of the inductive transducer located at the turbine shroud. The mass flow rate was measured with a calibrated pitot tube in the inlet duct.

Tests were conducted with an unmodified impeller and the performance map obtained. Tests were made at 17,000,

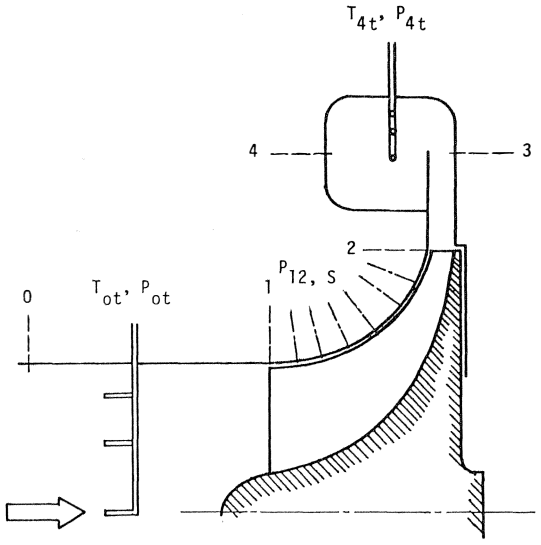

T_{ot}: Inlet stagnation temperature

T_{4t}: Collector exit stagnation temperature

P_{ot}: Inlet stagnation pressure

$P_{12, S}$: Compressor cover pressure

P_{4t}: Collector exit stagnation pressure

Figure 12. Schematic of Instrumentation.

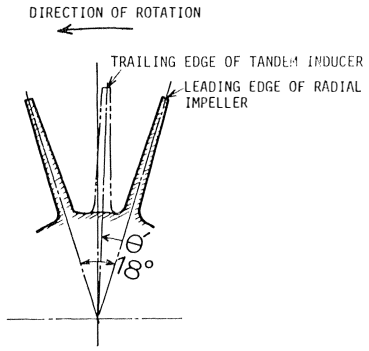

Figure 13. Definition of Offset.

20,000, and 23,000 RPM. The points located at the minimum flow rate for each operating line are those corresponding to the onset of violent surge.

The tests were then repeated with the modified impeller. For these tests, the tandem inducer was offset a value of -0.33, where the offset is defined as

$$\text{offset} = \frac{\theta'}{\dfrac{360^\circ}{\text{No. of blades}}}$$

θ' is shown in Figure 13. The offset in the direction of rotation is taken as positive. Figures 14 and 15 give a comparison of the efficiencies of the two impellers, and the pressure rise coefficients of the impellers, respectively.

These tests demonstrated that a tandem inducer reduces the amount of separation which occurs in impellers. This inducer design can be used to increase the efficiency of compressors with conventional unsplit diffusers. This also indicates that the present center positioning of splitter blades is in error.

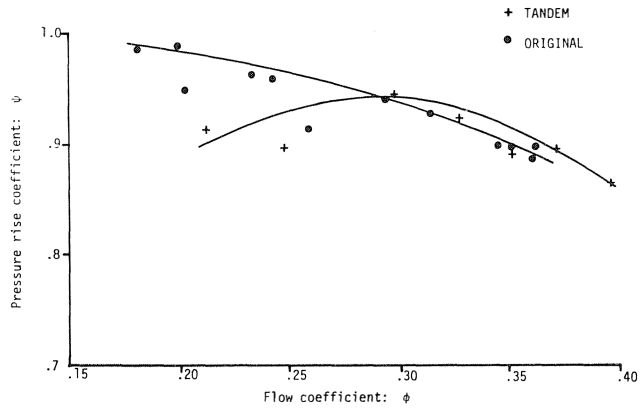

Figure 14. Comparison of Pressure Rise Coefficient Characteristics.

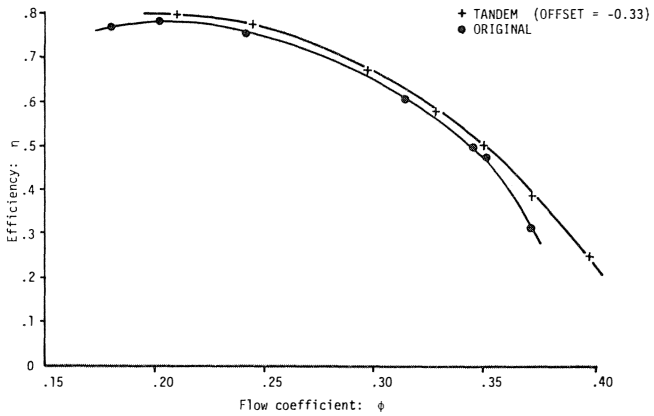

Figure 15. Comparison of Efficiency Characteristics.

OFF DESIGN PREDICTION

A program for developing a better method of detecting stall in centrifugal compressors resulted in a method for the theoretical prediction of off-design performance, and established a criterion for predicting and classifying stall conditions. The theoretical results are in good agreement with those obtained from field tests. The surge prediction is based on flow conditions in the boundary layer adjacent to the shroud casing. Surge, defined as the lower limit of stable operation of a compressor, comprises the reversal of flow in the compressor.

Velocity profiles in the boundary layer of a compressor can be related to pressure gradient in a direction along the casing. This pressure gradient, in turn, is associated with the pressure rise through the compressor. The pressure rise in a compressor is dependent on the rotational speed, efficiency, and flow through an impeller. Thus, for a given flow and speed condition, there exists a definite velocity profile, at any given point in the boundary layer of the casing. A relationship was established between the slope of this profile and surge flow.

For a mathematical formulation of the problem of studying the boundary layer flow, adjacent to the shroud casing, a natural coordinate system, such as shown in Figure 16, rotating with the impeller at a constant angular velocity ω_p is chosen.

Navier-Stokes equations in directions along and normal to casing can, respectively, be written as

$$W_1 \frac{\partial W_1}{\partial x_1} - \left(\frac{W_2^2}{r} + 2\omega_p W_2 + \omega_p^2 r \right) \frac{\partial r}{\partial x_1} = -\frac{1}{\rho}\frac{\partial P}{\partial x_1} + \nu \frac{\partial^2 W_1}{\partial x_3^2} + \frac{1}{r}\frac{\partial r}{\partial x_3}\frac{\partial W_1}{\partial x_3}\nu \qquad (3)$$

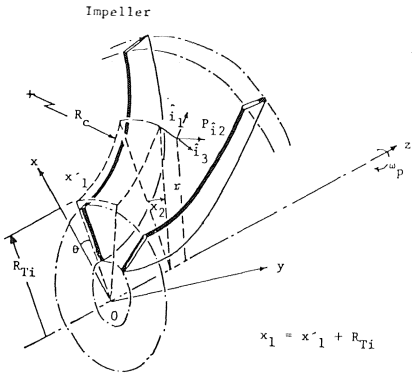

Figure 16. Natural Coordinate System.

and

$$\frac{W_1^2}{R_c} - \left(\frac{W_2^2}{r} + 2\omega_p W_2 + \omega_p^2 r\right)\frac{\partial r_1}{\partial x_3} = 0 \tag{4}$$

The continuity equation reduces to

$$\frac{\partial}{\partial x_1}(\rho r W_1) = 0 \tag{5}$$

The energy equation takes the form

$$W_1\frac{\partial T}{\partial x_1} = \frac{W_1}{\rho C_p} + \frac{\nu}{C_p}\left[\left(\frac{\partial W_1}{\partial x_3}\right)^2 + \left(\frac{\partial W_2}{\partial x_3} - \frac{W_2}{r}\frac{\partial r}{\partial x_3}\right)^2\right] \tag{6}$$

Equation of state is given by

$$P = \rho R' T \tag{7}$$

A simultaneous solution of equations (3) through (7) yields a differential equation of W_1 in x_3, as given below:

$$\frac{\partial^2 W_1}{\partial x_3^2} + B\frac{\partial W_1}{\partial x_3} + CW_1^2 + D' = 0 \tag{8}$$

The boundary conditions for equation (8) are the following.

At any given x_1,

$$\left.\begin{aligned} W_1(x_3 = 0) &= 0 \\ W_1(x_3 = \delta) &= W_{1\infty} \end{aligned}\right\} \tag{9}$$

and

Integrating equation (8) with respect to x_3 between the limits of 0 and δ, we get

$$\left.\frac{\partial W_1}{\partial x_3}\right|_{x_3=0}^{\delta} + B\,W_1\Big|_{x_3=0}^{\delta} + C\int_0^{\delta} W_1^2\,dx_3 + D'\,x_3\Big|_{x_3=0}^{\delta} = 0 \tag{10}$$

Using the value of the shear stress at the casing, equation (10) transforms to a polynomial in δ,

$$\delta^2\left(\frac{7C}{9}W_{1\infty}^2 + D'\right) + \delta(BW_{1\infty}) - \delta^{6/7}\left(\frac{0.0274 W_{1\infty}^{13/7}}{\nu^{6/7}}\right) + \frac{W_{1\infty}}{10} = 0 \tag{11}$$

A simplified solution yields

$$\delta(x_1) = \frac{4.545\,\nu}{W_{1\infty}(x_1)} \tag{12}$$

The slope of the velocity profile at the edge of the boundary layer can be given as

$$\left.\frac{\partial W_1}{\partial x_3}\right|_{x_3=\delta} = 0.022\,\frac{W_{1\infty}^2}{\nu} \tag{13}$$

The factor,

$$\tau_{surge} = \frac{1}{N_S}\cdot\frac{\nu\left.\frac{\partial W_1}{\partial x_3}\right|_{\delta}}{\left(\frac{U_e}{\sqrt{T_{ti}}}\right)^2} \tag{14}$$

termed the surge factor for convenience, is seen, as a result of the present analysis, to attain a definite value below which the centrifugal compressor goes into surge. In the case of shrouded impellers, the same analysis holds. The boundary layer considered is the one that is attached to the inside wall of the impeller shroud.

Prediction of the surge line using the concept of the surge factor developed here has been fairly accurate as seen from Figures 17 and 18. Some discrepancies in the lower aerodynamic speeds region of the compressor map in Figure 18 can be noted. This should, however, be observed in view of the experimental limitations in identifying the onset of surge, especially in higher pressure ratio compressors. While developing the theoretical program, the Laboratories also initiated a program to develop an instrumentation system for predicting the onset of surge in compressors. The system monitors the boundary layer and detects flow reversal in the boundary layer. Initial tests with this system installed in a gas pipeline compressor proved this system to be more responsive than existing surge detection systems. More extensive tests are planned to determine the optimum design and location for the monitoring probe.

COMBUSTOR

Combustor design is important in attaining adequate fuel economy, extended life of the hot section, and low emission levels, as well as achieving fuel flexibility. Combustion studies

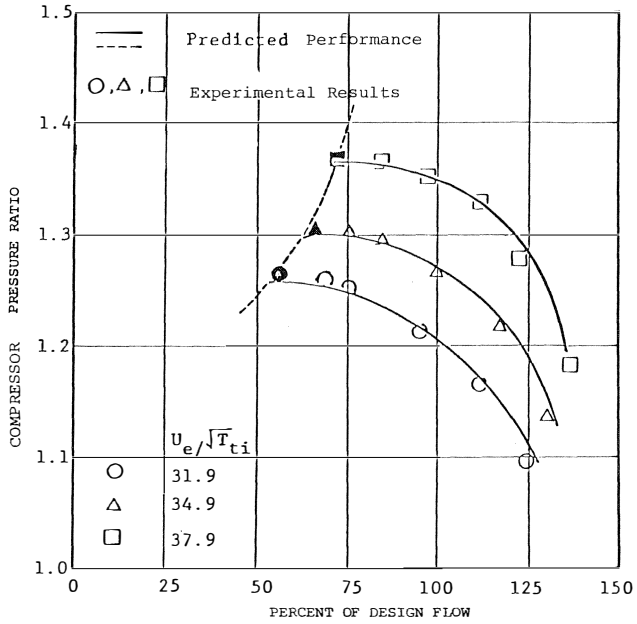

Figure 17. Comparison of Predicted Performance and Experimental Results.

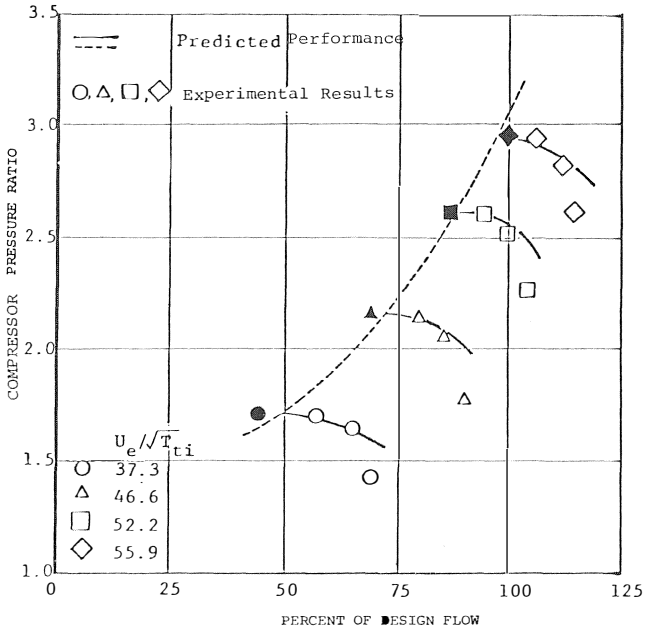

Figure 18. Comparison of Predicted Performance and Experimental Results.

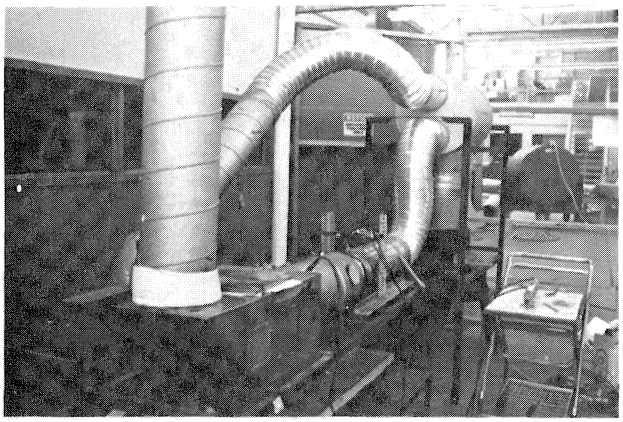

Figure 19. Combustion Facility Constructed With Aircraft Type Jet Engine Combustion Can.

at the Gas Turbine Laboratories have included improving combustor efficiency, emission levels and fuel capability.

Test Facilities

Test facilities available at the laboratories are two combustion rigs fully instrumented. The rigs were both made by removing one can from a can-annular type combustor. One test rig, Figure 19, made from an aircraft type gas turbine is of the straight-through flow design. The other, Figure 20, made from an industrial type gas turbine, is a reverse flow type. In both cases, the equipment may be considered as comprising three sections: (1) the air, fuel, and steam supply, (2) the combustion chamber, and (3) the exhaust duct and combustion gas sampling.

Air is supplied by belt driven centrifugal blowers. The air supply is controlled by damper valves and pulley size. Various fuels can be tested. Mapp, an industrial gas available in cylinders, is often used because of its safety and easy control by a gas regulator. Natural gas and other fuels can be used, but require special handling and control.

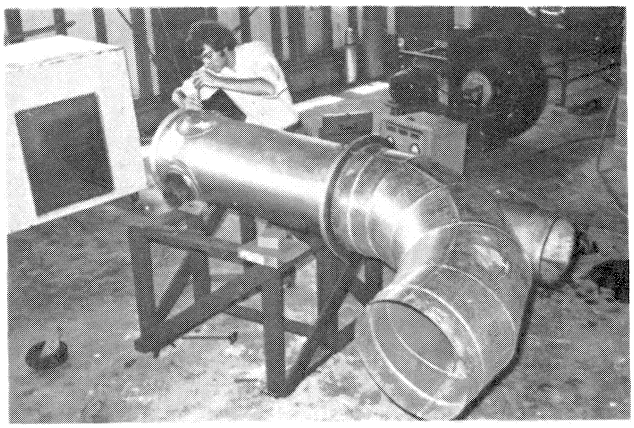

Figure 20. Combustion Facility Constructed With Industrial Type Gas Turbine Combustion Can.

The combustion section in both rigs is a commercial can and liner. One can was outfitted with a port allowing view into the primary combustion zone. Both cans are simply mounted to readily allow liner changes. Each rig is instrumented with thermocouples to allow gas as well as liner temperature measurement.

The exhaust duct in each case is fabricated from high grade stainless steel designed to adapt to the existing combustor can. Emission levels are monitored by an infrared analyzer.

CURRENT RESEARCH

NO_x Reduction

Recently a project attempting to reduce NO_x emission was completed. Flame temperature and the accompanying NO_x emissions were reduced by two different methods. One method employed a combustion liner redesign to achieve increased exhaust gas recirculation. The other method utilized a catalyst, in this case steam. Two different liner modifications were tested. In model 1, four ¾ inch-diameter pipes directed toward the nozzle caused inlet air to flow forward and form a vortex. The vortex suction increased the degree of recirculation and eliminated high temperature rich pockets. In the model 2 liner, an inner cyclinder, 4.5 inches long and 6 inches in diameter, was placed inside the liner to provide an annular space for combusted gases recirculating. A ring of 7.5 inch outer diameter and 5 inch inner diameter was also placed an inch beyond the inner cyclinder in order to expedite the recirculation. Figure 21 shows this modification. The results show that at the higher range of fuel air ratio NO_x production was lowered. Also, both modifications of carbon monoxide output was below that of the baseline combustor.

The injection of steam into the combustion primary zone predates the environmental concerns of the present decade. Steam, as inert gas and heat source, has the advantage of increasing turbine power and thermal efficiency, as shown in Figure 22 by Boyce and Chen, and also of decreasing the NO_x production. Steam fuel ratios between .25 and 1.25 were run at constant air fuel ratio of .0057. The result was a 40% reduction of NO_x at steam-fuel ratio of 1, however, carbon monoxide was increased 12%, as seen in Figure 23.

MULTIPLE FUELS

In the area of multiple fuels both inhouse experimental and field studies, with the aid of turbomachinery users' data, are underway. For experimental studies, one rig has a test

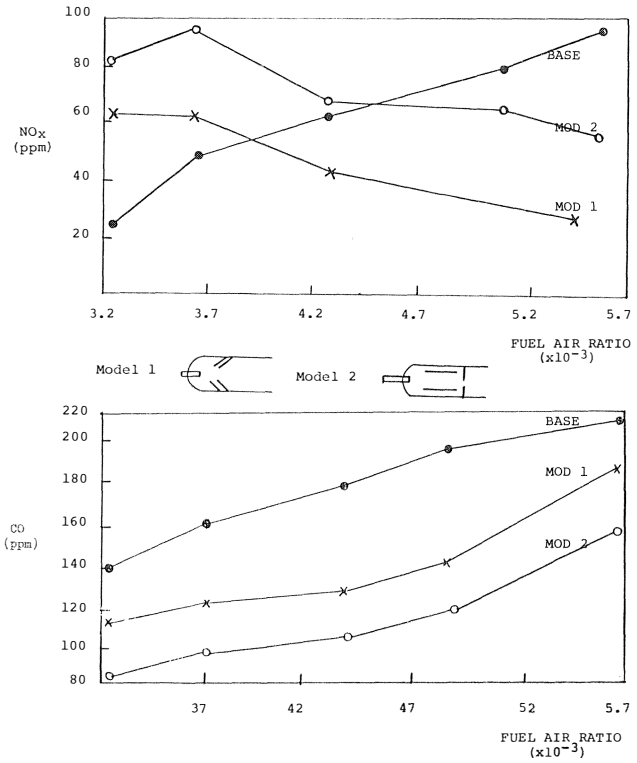

Figure 21. Results of Liner Modications to Reduce NO_x.

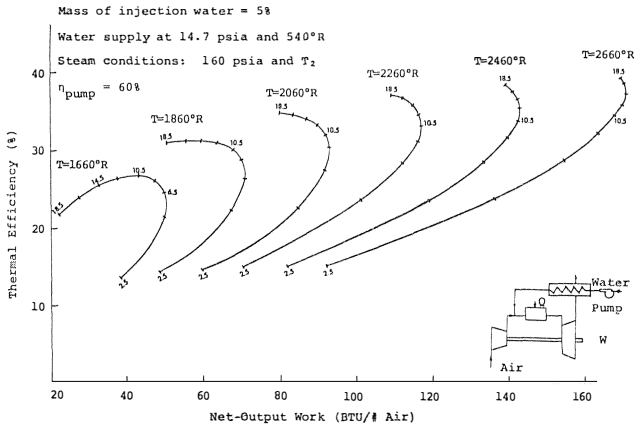

Figure 22. Performance Map of a Steam Injection Cycle.

section into which specimens are placed for corrosion studies. The other has a factory supplied fuel nozzle permitting exact duplication of fuel injection patterns. The field service data study involved determining economics and practicality of multi-fuel operation.

Due to the inherent fuel flexibility of gas turbine combustion, fuel candidates encompass the entire spectrum from gases to solids. Gaseous fuels include natural gas, process gas, and in the future, low BTU coal gas, while pulverized coal is being studied as a solid fuel. However, liquid fuel is generally implied when multifuel is discussed. Liquid fuel can vary from the light volatile naptha through kerosene to heavy viscous residual. Each class of liquid fuel has its own properties that require special attention.

The classes of liquid fuels and their requirements are shown in Table I. True distillates are ideal turbine fuels equal to natural gas. Naptha, due to its high volatility, may require a

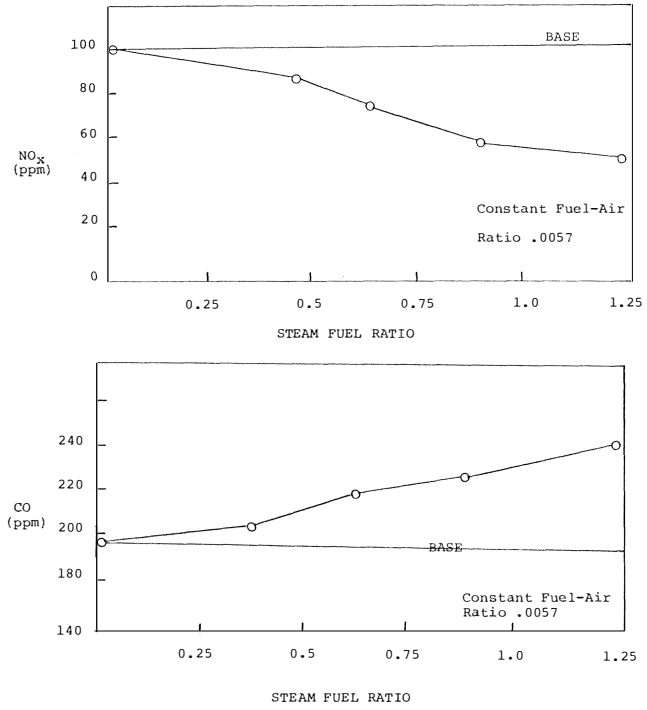

Figure 23. Results of Steam Injection to Reduce NO_x.

fuel tank with a floating head. As long as properties fall within specific limits, no special treatment is necessary. On occassion, the properties of a residual or crude can be made acceptable by blending.

Important properties of a liquid fuel to be considered are viscosity and ash content. The viscosity affects the fuel handling and injection design, while ash affects the necessary fuel treatment.

Viscosity is a measure of resistance to flow and is important in the design of fuel pumping systems. Ash can be present in two forms: (1) as solid particles designated sediment, and (2) oil or water soluble traces of metallic compounds. Sediment leads to fouling of the fuel system and obstruction of the fuel filter. The metallic compounds present in the ash are related to the corrosion and deposition properties of the fuel.

Trace elements of prime concern are: vanadium, sodium, potassium, lead, and calcium. Sodium and potassium are restricted because they react with sulfur at elevated temperatures to corrode metals by hot corrosion or sulfidation. Acceleration oxidation of the blades also occurs when liquid vanadium is deposited on the blade. Lead can cause corrosion but is not encountered often. Its presence is due mainly to contamination by leaded fuel or as a result of some refining practice. Calcium does not promote corrosion, but leads to hard deposits on the blading.

Corrosion mechanisms are not fully understood, however, it is known that corrosion rates are influenced by temperature. The corrosive threshhold is generally accepted to be in the 1100-1200° range. The relation between the temperature and concentration of sodium and vanadium is shown in Figure 24. How sodium and vanadium reduce life can be seen in Figure 25. Both figures show that increasing sodium accelerates corrosion faster than increasing vanadium.

FULL TREATMENT

If high ash fuels are to be utilized, corrosion protection must be achieved. The corrosion agents encountered most

TABLE 1. COMPARISON OF LIQUID FUELS FOR GAS TURBINES

General Fuel Type	True Distillate and Naphthas	Blended Heavy Distillates and Low Ash Crudes	Residuals and High Ash Crude
Fuel pre-heat	No	Yes	Yes
Fuel atomization	Mech/LP air	HP/LP air	HP air
Desalting	No	Some	Yes
Fuel inhibition	Usually none	Limited	Always
Turbine washing	No	Yes except distillate	Yes
Startup fuel	With naphtha	Some fuels	Always
Base fuel cost	Highest	Intermediate	Lowest
Description	High quality distillate essentially ash free	Low ash, limited contaminant levels	Low volatility, high ash
Types of fuels included	True distillates (naphtha, kerosene, No. 2 diesel, No. 2 fuel oil, JP-4, JP-5)	High quality crudes, slightly contaminated distillates, Navy distillate	Residuals and low grade crude (No. 5 fuel, No. 6 fuel, bunker C)
ASTM designation	1-GT, 2-GT, 3-GT	3-GT	4-GT
Turbine inlet temperature	Highest	Intermediate	Lowest

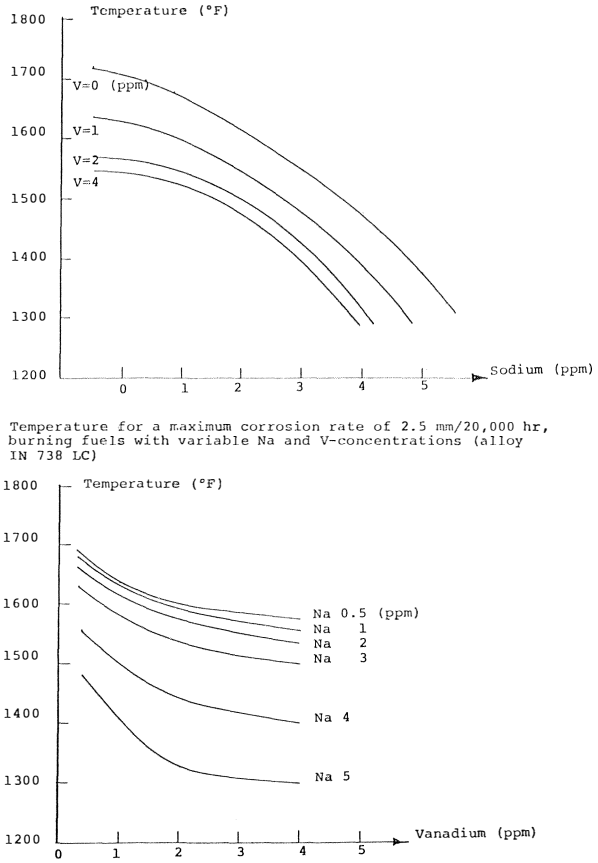

Figure 24. Corrosion as a Function of Fuel Impurities and Turbine Temperature.

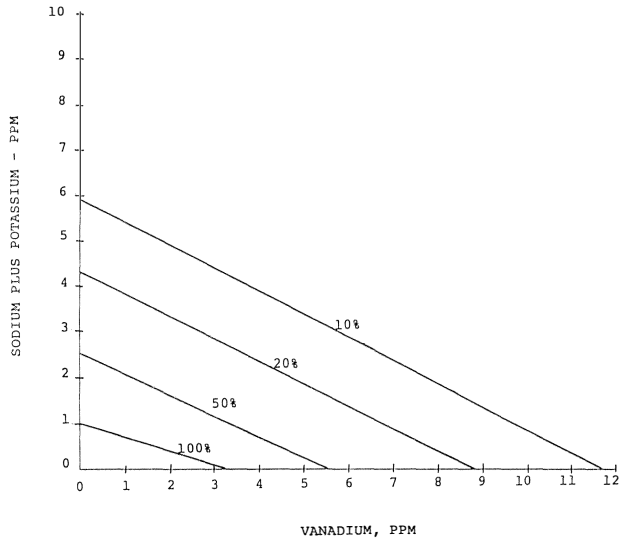

Figure. 25. Corrosive Effects of Trace Elements in Fuel.

TABLE 2. SELECTION OF FUEL WASHING SYSTEMS

Fuel	Washing System
Distillate	Centrifugal or DC electrostatic desalter
Heavy distillates	Centrifugal or AC electrostatic desalter
Light-medium crudes	Centrifugal or AC electrostatic desalter
Light residual	Centrifugal or AC electrostatic desalter
Heavy crudes	Centrifugal desalter and hybrid systems
Heavy residuals	Centrifugal desalter and hybrid systems

often are vanadium and sodium. Vanadium originates as a metallic compound in crude oil and is concentrated by the distillation process into the heavy oil fractions. Sodium compounds are most often present in the form of salt water, and can result from salty wells, transport over sea water, or mist injestion in an ocean environment. The methods used to treat the fuel are washing and the addition of additives.

Fuel washing relies on the water solubility to remove the salt and reduce the sodium, potassium, and calcium. Washing entails adding water, mixing to assure dissolving of the compounds, and removing the water. The water, containing the dissolved salts, can be removed by centrifuge, electrostatic separation, or a hybrid combination. The selection of the fuel washing system is influenced by the fuel type and is summarized in Table II.

Vanadium compounds are oil soluble and are thus unaffected by fuel washing. Without additives, vanadium forms low melting temperature compounds which deposit on the blade as

TABLE 3. COMPRESSOR DIAGNOSTICS

	η_c	P_2/P_1	T_2/T_1	Vibration	ΔT Bearing	Bearing Pressure	Bleed Chamber Pressure
Surge	↓	Variable	–	Highly fluctuating	↑	↑	Highly fluctuating
Fouling	↓	↓	↑	↑	–	–	–
Damaged blade	↓	↓	↑	↑	–	–	Highly fluctuating
Bearing failure	–	–	–	↑	↑	↓	–

a molten slag causing rapid corrosion. However, by the addition of a suitable compound, magnesium for example, the melting point of the vanadates is sufficiently increased to prevent them from being in the liquid state under service conditions.

The elevated melting point of the new compounds does lead to increased deposits thus lending more attention to cleaning and maintenance. This aspect will be discussed later.

FUEL INJECTION

A study presently underway seeks to relate combustor performance and fuel injection. By determining the optimum injection and pressure, a more efficient combustor can be designed. Since combustor velocity affects primary zone recirculation intensity and thus flame stabilization, it is held constant. Fuel injection angle and pressure are varied until optimum combustor performance is attained. Combustor performance is based on thermal efficiency, uniformity of outlet profile, liner temperature and emission levels.

MAINTENANCE

The necessary maintenance is affected by the unit environment and fuel quality in conjunction with the integrity of the design. Scheduling maintenance shut downs and predicting problem areas is dependent upon effective monitoring. Vibration, temperature, pressure, and sound should be monitored as well as fuel contaminates and air-borne sodium to assure proper diagnosis.

COMPRESSOR ANALYSIS

By monitoring the parameters mentioned above, it is possible to predict the following:

Clogged Air Filter — A clogged air filter may be detected by noting an increase in the pressure drop through the filter.

Compressor Approaching Surge — By using a boundary layer probe, it is possible to detect a flow reversal in the boundary layer before the unit actually surges. This concept is still being developed: however, it does have great promise.

Compressor Surging — Surge may be detected by noting a rapid increase in shaft vibration, along with a rapidly fluctuating pressure ratio. If more than one stage is present, the probes located within the bleed air chambers are useful in locating the problem stage.

Since the response time of a pressure transducer is less than 10 milliseconds, they may be used to detect a rotating surge condition. When this is present, there will be a pressure variation at some harmonic of the blade passage frequency.

If tip surge is present, the rake pressure probe will detect only a small pressure change, while the probes located along the shroud will indicate a rapidly fluctuating pressure.

Compressor Fouling — This is indicated by a decrease in pressure ratio accompanied by an increase of exit temperature and shaft vibration with time. The change in the temperature and pressure ratio tend to show a decrease in efficiency. If a change in vibration has occurred, the fouling is critical.

Damaged or Fluttering Compressor Blade — A sharp increase in shaft vibration and exit temperature over a short period of time indicates this problem. If more than one stage is present, it is possible to determine which stage experienced the failure by noting which frequency experienced the vibration increase.

Bearing Failure — Symptoms of bearing trouble include a loss of pressure, an increase in the temperature difference across the bearing and an increase in vibration. If oil whirl is present, there will be a vibration frequency corresponding to one half the running speed.

These problems are summarized in Table III.

COMBUSTOR ANALYSIS

Due to limited probe life in the combustor, the only two parameters which can be measured are fuel pressure and evenness of combustion.

Plugged nozzle — This is indicated by an increase in fuel pressure in conjunction with increased combustion unevenness. This is a common problem when residual fuels are used.

Cross-over tube failure — This is indicated by unevenness of combustion, which may be measured with an acoustic meter.

These problems are shown in Table IV.

TURBINE ANALYSIS

Turbine Fouling — This is indicated by an increase in turbine exhaust temperature, accompanied by a sudden change in vibration amplitude.

Damaged Turbine blades — This results in a large vibration increase accompanied by an increase in the exhaust temperature.

Nozzle Bowed — The exhaust temperature will increase and there may be an increase in vibration noted at the excitation frequency of the first stage.

TABLE 4. COMBUSTOR DIAGNOSTICS

	Fuel Pressure	Unevenness of Combustion (Sound)
Nozzle clogging	↑	↑
Combustor fouling	–	↑
Crossover tube failure	–	↑

TABLE 5. TURBINE DIAGNOSTICS

	η_t	P_3/P_4	T_3/T_4	Vibration	ΔT Bearing	Cooling Air Pressure	Wheel Space Temperature	Bearing Pressure
Fouling	↓	–	↓	↑	–	–	↑	–
Damaged blade	↓	–	↓	↑	–	–	–	–
Bowed nozzle	↓	↓	↓	↑	–	–	↑	–
Bearing failure	–	–	–	↑	↑	–	–	↓
Cooling air failure	–	–	–	–	↑	↓	↑	–

TABLE 6. OPERATION AND MAINTENANCE LIFE OF AN INDUSTRIAL TURBINE

Type & Number Load, Fuel & Starts		Type Inspection – Hrs. of Operation			Expected Life (Replacement) – Hrs. of Operation		
		Service	Minor	Major	Comb. Liners	1st Stage Nozzle	1st Stage Buckets
BASE							
	*	+	+	+	+	+	+
Natural gas	1/1000	4500	9000	28000	30000	60000	100000
Natural gas	1/10	2500	4000	13000	7500	42000	72000
Distillate oil	1/1000	3500	7000	22000	22000	45000	72000
Distillate oil	1/10	1500	3000	10000	6000	35000	48000
Residual	1/1000	2000	4000	5000	3500	20000	28000
Residual	1/10	650	1650	2300			
SYSTEM PEAKING x							
Natural gas	1/10	3000	5000	13000	7500	34000	
Natural gas	1/5	1000	3000	10000	3800	28000	
Distillate	1/10	800	2000	8000			
Distillate	1/5	400	1000	7000			
TURBINE PEAKING x							
Natural gas	1/5	800	4000	12000	2000	12000	
Natural gas	1/1	200	1000	3000	400	9000	
Distillate	1/5	300	2000	6000			
Distillate	1/1	100	800	2000			

* 1/5 = One start per five operating hours.

x No residual usage due to low load factor and high capital cost.

BASE = Normal maximum continuous load.

SYSTEM PEAKING = Normal maximum load of short duration and daily starts.

TURBINE PEAKING = Extra load resulting from operating temperature 50° to 100°F above base temperature for short durations.

SERVICE = Inspection combustion parts, required downtime approximately 24 hours.

MINOR = Inspection of combustion plus turbine parts, required downtime approximately 80 hours.

MAJOR = Complete inspection and overhaul, required downtime approximately 160 hours.

Note: Maintenance times are arbitrary and depend on manpower availability and training, spare parts and equipment availability, and planning. Boroscope techniques can help reduce downtime.

Bearing failure — The symptoms of bearing problems for a turbine are the same as for a compressor.

Cooling air failure — Problems associated with the blade cooling system may be detected by an increase in the pressure drop in the cooling line and by a change in the vibration frequency associated with the first stage, that being the stage which is usually cooled. Problems summarized in Table V.

Table VI indicates the expected operational life of a gas turbine hot section. The life figures in this table are for industrial type turbines, and the data was collected from users of

various heavy duty turbines. Careful inspection reveals that the number of starts per operational hour is as important a life factor as the fuel used, natural gas or diesel.

The deposition problem with heavier fuels was mentioned earlier, but left as a maintenance problem. Monitoring can detect turbine deposit build-up and alert an engineer to the necessity of a "fix." The problem is best alleviated by turbine, and in the case of intake contaminants, compressor cleaning or washing.

Dry cleaning is achieved by injecting a mild abrasive into the turbine or compressor. Possible abrasives include walnut shells, rice and spent catalyst. Dry cleaning can remove up to 50% of the deposits without requiring a shutdown. If this does not restore sufficient power shutdown and water wash is necessary. Depending on the ash present in the fuel, continuous operation on the ash bearing fuels varies from 150 to 1500 hours. Figure 26 shows the effect of turbine deposits on output power. The amount of ash in the fuel will effect the maintenance costs. This is shown in Table VII.

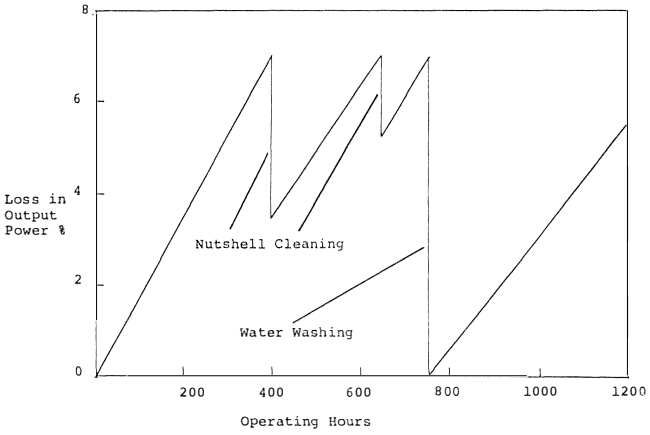

Figure. 26 Effects of Cleaning on Power Output.

A study of multi-fuel operation based on users' field data was also carried out. A summary of service problems and their frequency is shown in Table VIII. One year's operating experience with liquid fuels is summarized in Table IX. This table presents fuel type, operating data, and service problems.

TABLE 7. AVERAGE TOTAL MAINTENANCE AND COST FACTORS FOR GAS TURBINES

Fuel	Expected Actual Maintenance Cost Mills/Kwh	Expected Maintenance Cost Factor
Natural gas	0.3	1.0 = base line
No. 2 distillate oil	0.4	1.25
Typical crude oil	0.6	2.0
No. 6 residual oil	1.0	3.33

TABLE 8, SUMMARY OF 1974 GAS TURBINE USERS' DATA FOR LIQUID FUEL TURBINES

Major Problem Areas in Order of Frequency	Number of Occurrences	Percent of Total Liquid Units
Flame detector (Malfunction or failed)	5	19
Combustor liner failure	4	15
Deposits fuel nozzles	4	15
Control problems	4	15
Deposits on turbine nozzle	3	11.5
Combustor liner burning	3	11.5
Cracked transition pieces	3	11.5
Fuel system failure	3	11.5
Total number of liquid fuel units	26	
Percent of total units	7.2%	

TABLE 9, LIQUID FUEL EXPERIENCE–1974

Maker	Fuel	Application	Temp Fire	Exh	Hours	Load	Use	Avail	Rel	Fuel Related Problems
Ruston	Dual gas-diesel	Gen. drive		925		50	50	100%	100%	Hi press at nozzle, flame, detector fog up false signals.
Ruston	Diesel	Pump					65%			Diesel requires annual overhaul, auto start to be installed to reduce burning, extend overhaul.
GE	Refinery fuel	Process compr	1500	975		98	94	94		Sticking second stage nozzles, fuelgas regulator.
Ruston	Diesel	Power	1420	980	59000	85	60	88	90%	Corrosion 1st CT stators on oil at 30000 hr.
Ruston	Diesel	Pump drive	1540	980	200C	88	40	90	90%	
Ruston	Diesel	Power	1455	932	7300	67.5	69.7	94.2	99.2	
Ruston	Gas oil	Power	1427	932	10800	50%	33.33	95	98	Flame failure unit, cause most trips.
Ruston	Dual distillate	Pumps		875	400					Flame detectors fail-leaking fuel solenoid. Excessive carbon build-up on burners after short running periods.
GE	Crude	Pump		815					98.5	Comb liner burning due to liquid fuel.
GE	No. 2 oil	Compression	1450	850	120000	100	74	87.2	88.3	Cleaned fuel nozzles.
GE	No. 2 oil	Compression	1450	850	120000		71	88.8	91.2	Major overhaul, fuel nozzles, back fire in fuel gas line.
GE	Diesel	Pump			2950	100	86		60	Burnt comb. liners, distillate fuel system not working, flame detector cause trip.
GE	No. 2 oil	Power	1560	700	11696	8.9	12.8	89.3	89.3	
GE	No. 2 oil	Power	1560	925	11047	9.4	12.4	91.1	91.3	Control
GE	No. 2 oil	Power	1560	925	6800	10.4	13.5	87.0	88.3	
GE	Light crude	Generator		935	22744					See insert.
GE	No. 2 diesel	Power	1600	860	61317	Base	100			Control
GE	Gas and oil	Power		890	10000	85.8	89.1	92.6	94.7	Plugged fuel nozzles.
GE	Gas and No. 2 diesel	Power		930	13600		64.3	64.3	100%	Control (fuel changing).
GE	Kerosene	Compr	1650	905	17300		94	94	97.2	Smokeless com can failed–broke can, trans. pcs., 1st stage nozzle.
GE	Kerosene	Compr		925	610		15.4	98.9	99.6	
Solar	No. 2 diesel	Power	1410	860		60	65	85	99%	
Westinghouse 501G	No. 2 fuel oil	Power			3200	10.5	12.2	82.2	85.9	Basket life as short as 250 hrs.
Westinghouse 251AA	No. 2 fuel oil	Power			4000	5.3	6.4	81.6	97.7	Cracking in burner.
Westinghouse W-191-6	No. 2 diesel	Power	1450	780	45400	80.3	86.3	87.3	98.5	
Mitsubishi	No. 2 diesel	Generator	1450	801	11500		91	91	98.7	Comb temp detector burnt trans. pcs cracked.

$$\text{Load Factor} = \frac{\text{Developed BHP Hours}}{\text{Installed BHP x Onstream Hours}} \times 100\%$$

$$\text{USE Factor \%} = \frac{\text{Fired Hours}}{\text{Installed Hours}} \times 100$$

$$\text{Availability \%} = \frac{\text{Installed Hours} - (\text{Scheduled} + \text{Unscheduled Outage})}{\text{Installed Hours}} \times 100$$

$$\text{Reliability \%} = \frac{\text{Installed Hours} - \text{Unscheduled Outage}}{\text{Installed Hours}} \times 100$$

INSERT – CRUDE OIL

Combustor inspected every 3500 - 4000 hours.

Nozzle–had typical carbon build-up, soft, thin.

Liners–typical deposits liners, were cleaned and reinstalled. One liner had two cracks between lower close to fire tube hole.

Transition–no crack, large deposits, replaced at 11242 hrs.
1st Stage Nozzle–extremely heavy deposit, no evidence of cracks.
2nd Stage Nozzle–deposits not as heavy.

REFERENCES

1. Katsanis, T., "Use of Arbitrary Quasi-Orthogonals for Calculating Flow Distribution in the Meridional Plane of a Turbomachine," NASA TN D-2546 Dec. 1964.
2. Boyce, M. P. and Bale, Y. S., "A New Method for the Calculations of Blade Loadings in a Radial Flow Compressor," ASME Paper No. 71-GT-60.
3. Senoo, Y. and Nakase, Y., "An Analysis of Flow Through a Mixed Flow Impeller," ASME Paper No. 71-GT-2.
4. Senoo, Y. and Nakase, Y., "A Blade Theory of an Impeller with an Arbitrary Surface of Revolution," ASME Paper No. 71-GT-17.
5. Bale, Y. S., "Blade Loading Analysis of a Centrifugal Impeller Using Viscous Effects," Ph.D. Dissertation, Texas A&M University, Dec. 1975.
6. Boyce, M. P., "A Practical Three-Dimensional Flow Visualization Approach to the Complex Flow Characteristics in a Centrifugal Impeller," ASME Paper No. 66-GT-83.
7. Fowler, H. S., "An Investigation of the Flow Processes in Centrifugal Compressor Impeller," National Research Council of Canada, Rep. ME-229, Ottawa, 1969.
8. Fowler, H. S., "Experiments on the Flow Processes in Simple Rotating Channels," NRCC ME-229, Ottawa, January 1969.
9. Bammert, K. and Rautenberg, M., "On the Energy Transfer in Centrifugal Compressors," ASME Paper No. 74-GT-121.
10. Gorton, C. A. and Lakshminarayana, B., "A Method of Measuring the Three-Dimensional Mean Flow and Turbulence Quantities Inside a Rotating Turbo-machinery Passage," ASME Paper No. 75-GT-4.
11. Mizuki, S., Ariga, J., and Watanabe, I., "A Study on the Flow Mechanism Within Centrifugal Impeller Channels," ASME Paper No. 75-GT-14.
12. Eckardt, D., "Detailed Flow Investigations Within a High-Speed Centrifugal Compressor Impeller," ASME Paper No. 76-FE-13.
13. Balje, O. E., "Axial Cascade Technology and Application to Flow Path Designs. Part I — Axial Cascade Technology," Trans. ASME, Series A, Vol. 90, No. 4, Oct. 1968, pp. 309-328.
14. Prithvi Raj, D. and Narayanan, R., "Studies on a Centrifugal Pump with Tandem Vanes," ASME Paper No. 74-FE-32.